

## BER Performance of Uplink NOMA With Joint Maximum-Likelihood Detector

Jeong Seon Yeom <sup>1</sup>, Student Member, IEEE,  
 Han Seung Jang <sup>2</sup>, Member, IEEE, Kab Seok Ko <sup>3</sup>, Member, IEEE,  
 and Bang Chul Jung <sup>4</sup>, Senior Member, IEEE

**Abstract**—We mathematically derive an upper bound of bit-error rate (BER) of uplink non-orthogonal multiple access (NOMA) systems with quadrature phase shift keying (QPSK) modulation in fading channels. In particular, we exploit the joint maximum-likelihood (ML) detector at a base station (BS) with multiple antennas since it results in the optimal BER performance of a super-imposed QPSK modulated symbols from multiple users. In particular, we obtain a closed-form integral of Q-function with Erlang distributed random variable to derive the BER. We also obtain diversity order of the uplink NOMA systems. Through extensive computer simulations, we validate that our analytical results match well with the simulation results especially in high signal-to-noise ratio (SNR) regime.

**Index Terms**—Non-orthogonal multiple access (NOMA), bit-error rate (BER), fading channels, joint maximum-likelihood (ML) detection, multiple antennas.

### I. INTRODUCTION

Non-orthogonal multiple access (NOMA) has been considered as an emerging technique to improve spectral efficiency, increase connection densities, or reduce latency for 5G wireless networks [1]. The NOMA technique is being proposed for 3GPP new radio (NR) standard, called 5G, as an essential component [2], [3]. NOMA techniques are classified into power-domain NOMA (PD-NOMA) and code-domain NOMA in general. In academia, performances of the NOMA technique have been analyzed in terms of sum-rate, outage probability, and bit-error rate (BER) in cellular networks. In [4] and [5], the ergodic sum-rate and the outage probability of the NOMA technique were investigated based on information theory in the downlink and uplink cellular network, respectively. In addition, the outage probability was mathematically analyzed for multi-input multi-output (MIMO) NOMA systems in both downlink and uplink cellular networks by considering signal alignment and power control techniques [6].

In comparison with the outage probability analysis in [4]–[7], a relatively small number of studies on the BER performance have been

conducted. In [8], an exact average BER expression of quadrature phase shift keying (QPSK) modulation was mathematically derived for uplink NOMA systems in an additive white Gaussian noise (AWGN) channel, which is not a practical assumption. In [9], the BER performance of QPSK modulation at both cell-edge user and cell-center user was analyzed for downlink NOMA systems in fading channels, assuming successive interference cancellation (SIC) at receivers. In [10], the BER performances of both downlink and uplink NOMA systems were investigated for fading channels by considering the SIC technique at receivers, where both base station (BS) and mobile stations (MSs) are assumed to be equipped with a single antenna. Even though previous studies on BER analysis of the NOMA systems considered the SIC technique at receivers [8]–[10], it was shown that the joint maximum-likelihood (ML) detector achieves the optimal performance in terms of error probability for the uplink NOMA systems over fading channels [11].

Recently, joint multiuser detection techniques were applied to NOMA systems [12], [13]. In [12], the pairwise error probability (PEP) of the uplink NOMA system was mathematically analyzed over fading channels, assuming multi-dimensional constellations and the joint ML detector. However, the closed-form solution was obtained only when all users (transmitters) are located at the same distance from the BS [12]. In [13], a novel codebook design method was proposed for a downlink sparse-code multiple access (SCMA) system with star-QAM constellations, assuming the message passing algorithm (MPA) at the receiver. In particular, the approximated BER of the SCMA is obtained in Rayleigh fading channels, where both the BS and MSs are assumed to be equipped with a single antenna [13], but the BER analysis cannot be extended to the uplink NOMA system with the multi-antenna BS that we consider in this paper.

In this paper, we mathematically analyze the BER performance of a two-user uplink PD-NOMA system in fading channels, assuming the joint ML detection technique instead of the SIC technique at the BS. We assume multiple antennas at the BS, which is quite practical in commercial cellular networks, and two users are located with arbitrary distance from the BS and they adopt QPSK modulation. Since it is hard to obtain the exact BER in closed-form, we derive an upper bound of the BER by using well-known union bound inequality. The mathematical analysis on the BER in this paper can be regarded as a generalized version of [12] in terms of user location perspective. Through extensive computer simulations, it is shown that the joint ML detector significantly outperforms the conventional SIC technique and the analytical results match well with the simulation results especially when the signal-to-noise ratio (SNR) is high.

The rest of this paper is organized as follows. In Section II, the system model of the uplink NOMA with joint ML detector is introduced. In Section III, we mathematically analyze the BER performance of cell-center and cell-edge user. The diversity order is also numerically analyzed in Section III-C and computational complexity of both SIC detector and joint ML detector is also compared in Section III-D. In Section IV, numerical results are shown. Finally, conclusions are drawn in Section V.

### II. SYSTEM MODEL

We consider an uplink NOMA system consisting of a BS with  $N$  antennas and two users with a single antenna as shown in Fig. 1. In this paper, we call a cell-center user (user C) the user having the larger

Manuscript received October 5, 2018; revised April 4, 2019 and July 14, 2019; accepted July 28, 2019. Date of publication August 5, 2019; date of current version October 18, 2019. This work was supported in part by the National Research Foundation through the Basic Science Research Program, funded by the Ministry of Science and ICT under Grant NRF-2019R1A2B5B01070697 and in part by the National Research Foundation, funded by the Korea government Ministry of Science and ICT under Grant NRF-2019R1F1A1061023. The review of this paper was coordinated by Dr. B. Natarajan. (Corresponding author: Bang Chul Jung.)

J. S. Yeom and B. C. Jung are with the Department of Electronics Engineering, Chungnam National University, Daejeon 34134, South Korea (e-mail: jsyeom@cnu.ac.kr; bcjung@cnu.ac.kr).

H. S. Jang is with the School of Electrical, Electronic Communication, and Computer Engineering, Chonnam National University, Yeosu 59626, South Korea (e-mail: hsjang@jnu.ac.kr).

K. S. Ko was with the Department of Electronics Engineering, Chungnam National University, Daejeon 34134, South Korea. He is now with the Qualcomm Institute, University of California San Diego, San Diego, CA 92093, USA (e-mail: chlingrc@gmail.com).

Digital Object Identifier 10.1109/TVT.2019.2933253

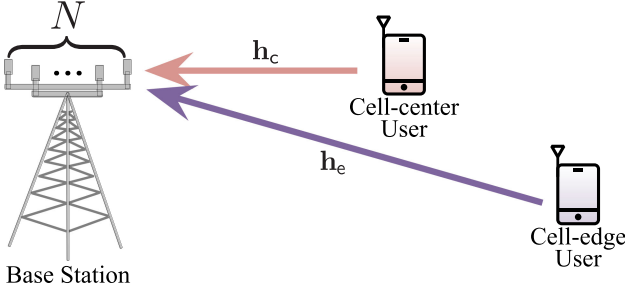


Fig. 1. System model of uplink NOMA consisting of a BS with multiple antennas and two users with a single antenna.

average channel gain, while we call a cell-edge user (user  $\Theta$ ) the user having the smaller average channel gain. Then, the received signal at the BS,  $\mathbf{y} \in \mathbb{C}^{N \times 1}$ , is given by

$$\mathbf{y} = \mathbf{h}_c \sqrt{P_c d_c^{-\alpha}} x_c + \mathbf{h}_e \sqrt{P_e d_e^{-\alpha}} x_e + \mathbf{n}, \quad (1)$$

where  $P_u$  ( $u \in \{\mathbf{c}, \Theta\}$ ) and  $d_u$  denote the transmit power and distance from the BS of user  $u$ , respectively. The term  $\alpha$  represents the path-loss exponent and  $\mathbf{h}_u \in \mathbb{C}^{N \times 1}$  denotes the wireless channel vector from user  $u$  to the BS. All elements of  $\mathbf{h}_u$  are assumed to follow identically and independently distributed (i.i.d.) complex Gaussian distribution with zero mean and unit variance, i.e.,  $\mathbf{h}_u \sim \mathcal{CN}(\mathbf{0}, \mathbf{I}_N)$ . The additive white Gaussian noise at the BS is denoted by  $\mathbf{n} \in \mathbb{C}^{N \times 1}$ , each element of which is i.i.d. complex Gaussian random variable with zero mean and variance of  $N_0$ . The term  $x_u \in \mathbb{C}$  denotes the transmitted modulation symbol of user  $u$ . The BS is assumed to know the channel gain vector from two users,  $\mathbf{g}_u$ , where  $\mathbf{g}_u \triangleq \mathbf{h}_u \sqrt{P_u d_u^{-\alpha}}$  for  $u \in \{\mathbf{c}, \Theta\}$ , i.e.,  $\mathbf{g}_u \sim \mathcal{CN}(\mathbf{0}, P_u d_u^{-\alpha} \cdot \mathbf{I}_N)$ . By definition  $d_e > d_c$ , but it is possible that  $\|\mathbf{g}_c\|^2 < \|\mathbf{g}_e\|^2$  due to small-scale fading effect. At the BS, the *optimal* joint ML detector is assumed in this paper, and then the estimate of both signals from two users is given by

$$[\hat{x}_c, \hat{x}_e] = \arg \min_{x_c, x_e \in \mathcal{X}} \|\mathbf{y} - \mathbf{g}_c x_c - \mathbf{g}_e x_e\|^2, \quad (2)$$

where  $\mathcal{X} = \{s_1, s_2, s_3, s_4\} = \{(1+j)/\sqrt{2}, (-1+j)/\sqrt{2}, (-1-j)/\sqrt{2}, (1-j)/\sqrt{2}\}$  since the QPSK modulation is adopted at users.

### III. BER PERFORMANCE ANALYSIS

In this section, we mathematically derive the upper bound of the average BER of both cell-center and cell-edge users. We first investigate the BER performance of user  $\mathbf{c}$  and then consider the BER of user  $\Theta$ .

#### A. BER of Cell-Center User

Fig. 2(a) shows the super-imposed QPSK symbols from two users at the BS, the QPSK mapping rule, and the error event of the cell-center user, where first two bits indicate the bits of user  $\mathbf{c}$  and other two bits indicate the bits of user  $\Theta$ . For convenience, we first consider the case that both users send all zero bits, i.e.,  $x_c = x_e = s_1 \triangleq (1+j)/\sqrt{2}$ , and we focus on obtaining BER of the *first* bit among two bits of user  $\mathbf{c}$ .<sup>1</sup> Then, the bit error occurs when the joint ML detector chooses one of green constellation points as the estimate for the transmitted symbol instead of black constellation point as shown in Fig. 2(a). Using the union bound and detection error probability in a complex vector

<sup>1</sup>We will show that the BER is unchanged regardless of both  $x_c$  and  $x_e$ , and it is the same for the second bit later.

space [14], the conditional BER for given  $\mathbf{g}_c$  and  $\mathbf{g}_e$  is upper bounded by

$$\Pr(\mathcal{E} | \mathbf{g}_c, \mathbf{g}_e) \leq \sum_{i=1}^8 Q \left( \sqrt{\frac{\delta_i^2}{2N_0}} \right), \quad (3)$$

where  $\delta_i = \|\mathbf{g}_c a_i + \mathbf{g}_e b_i\|$ ,  $a_i = s_1 - s_4$  for  $1 \leq i \leq 4$ ,  $a_i = s_1 - s_3$  for  $5 \leq i \leq 8$ ,  $b_i = s_1 - s_i$  for  $1 \leq i \leq 4$ , and  $b_i = s_1 - s_{i-4}$  for  $5 \leq i \leq 8$ . Then,  $\mathbf{g}_c a_i + \mathbf{g}_e b_i \sim \mathcal{CN}(\mathbf{0}, (P_c d_c^{-\alpha} |a_i|^2 + P_e d_e^{-\alpha} |b_i|^2) \cdot \mathbf{I}_N)$  due to property of complex Gaussian random vector. Let  $Z_i \triangleq \delta_i^2 / (2N_0)$ , and then  $Z_i$  follows Erlang distribution with mean  $N\gamma_i$  and variance  $N\gamma_i^2$ , where  $\gamma_i = (P_c d_c^{-\alpha} |a_i|^2 + P_e d_e^{-\alpha} |b_i|^2) / (2N_0)$ . Let us define the received SNR of two users at the BS as  $\rho_c = P_c d_c^{-\alpha} / N_0$  and  $\rho_e = P_e d_e^{-\alpha} / N_0$ . Then,  $\gamma_i$  can be rewritten by

$$\gamma_i = \frac{\rho_c |a_i|^2 + \rho_e |b_i|^2}{2}. \quad (4)$$

The probability density function of  $Z_i$  is given by

$$f_{Z_i}(z) = \frac{z^{N-1}}{(N-1)! \gamma_i^N} \exp\left(-\frac{z}{\gamma_i}\right). \quad (5)$$

We explicitly derive an upper bound of the average BER of user  $\mathbf{c}$  as follows:

$$\begin{aligned} P_{b,c} &\leq \mathbb{E} \left[ \sum_{i=1}^8 Q(\sqrt{Z_i}) \right] = \sum_{i=1}^8 \mathbb{E} \left[ Q(\sqrt{Z_i}) \right] \\ &\stackrel{(a)}{=} \sum_{i=1}^8 \int_0^\infty Q(\sqrt{z}) f_{Z_i}(z) dz, \end{aligned} \quad (6)$$

where (a) denotes the expectation (mean) of a continuous random variable [15]. Then, (6) is further derived as follows:

$$\begin{aligned} P_{b,c} &\leq \sum_{i=1}^8 \int_0^\infty Q(\sqrt{z}) f_{Z_i}(z) dz \\ &= \sum_{i=1}^8 \int_0^\infty \int_{\sqrt{z}}^\infty \frac{1}{\sqrt{2\pi}} \exp\left(-\frac{v^2}{2}\right) \frac{z^{N-1}}{(N-1)! \gamma_i^N} \exp\left(-\frac{z}{\gamma_i}\right) dv dz \\ &\stackrel{(b)}{=} \sum_{i=1}^8 \int_0^\infty \frac{1}{\sqrt{2\pi}} \exp\left(-\frac{v^2}{2}\right) \int_0^{v^2} \frac{z^{N-1}}{(N-1)! \gamma_i^N} \exp\left(-\frac{z}{\gamma_i}\right) dz dv \\ &= \sum_{i=1}^8 \int_0^\infty \frac{1}{\sqrt{2\pi}} \exp\left(-\frac{v^2}{2}\right) \left[ 1 - \exp\left(-\frac{v^2}{\gamma_i}\right) \sum_{k=0}^{N-1} \frac{v^{2k}}{k! \gamma_i^k} \right] dv \\ &= \sum_{i=1}^8 \frac{1}{2} \left[ 1 - \sum_{k=0}^{N-1} \binom{2k}{k} \sqrt{\frac{1}{1+2/\gamma_i}} \frac{1}{(2\gamma_i+4)^k} \right], \end{aligned} \quad (7)$$

where (b) represents the change of the order in double integrals. As we noted before, (7) denotes the BER of user  $\mathbf{c}$ 's first bit given that both users send  $s_1$ . From now, we will show that (7) is actually the unconditional BER of user  $\mathbf{c}$ 's first bit regardless of both  $x_c$  and  $x_e$ . Furthermore, we will show that the second bit of user  $\mathbf{c}$  has the same BER as well.

For given  $\mathbf{g}_c$  and  $\mathbf{g}_e$ , the BER in (7) depends on  $\gamma_i$ , and then  $\gamma_i$  depends only on a tuple<sup>2</sup>  $(|a_i|, |b_i|)$  for  $i = 1, 2, \dots, 8$ . The bit error occurs from 8 different error events, each of which depends on the tuple  $(|a_i|, |b_i|)$ . Thus, the another conditional BER when  $x_c$  or  $x_e$  is not equal to  $s_1$  can be derived by obtaining the corresponding tuple  $(|a_i|, |b_i|)$ . If

<sup>2</sup>A tuple is defined as a finite *ordered* list (sequence) of elements.

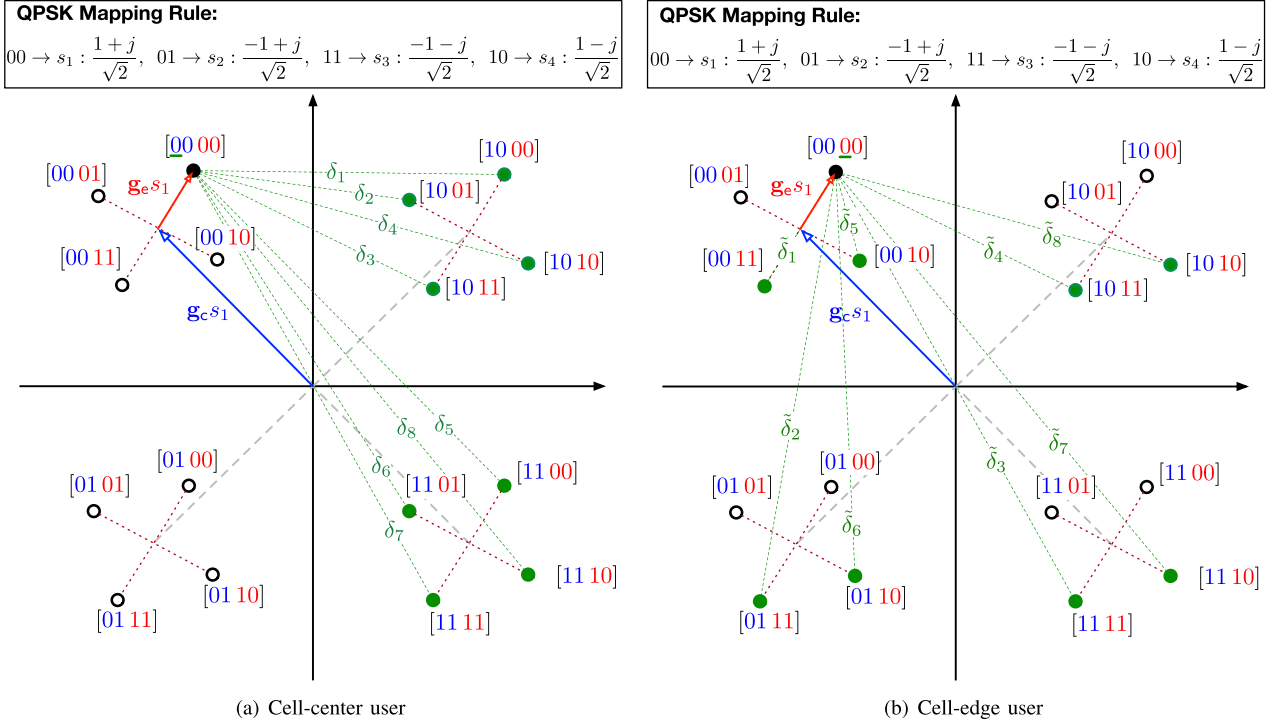


Fig. 2. Received signal model of super-imposed QPSK symbols from two users at the BS and error event, where  $\|\mathbf{g}_c\| > \|\mathbf{g}_e\|$ .

TABLE I  
ALL ELEMENTS OF  $\mathcal{T}_{l,m}^{c,t}$

$i$	$\mathcal{T}_{l,m}^{c,t}$				
	$\mathcal{T}_{1,1}^{c,1}$	$\mathcal{T}_{1,2}^{c,1}$	$\dots$	$\mathcal{T}_{4,3}^{c,2}$	$\mathcal{T}_{4,4}^{c,2}$
1	$(\sqrt{2}, 0)$	$(\sqrt{2}, \sqrt{2})$	$\dots$	$(2, 2)$	$(2, \sqrt{2})$
2	$(\sqrt{2}, \sqrt{2})$	$(\sqrt{2}, 0)$	$\dots$	$(2, \sqrt{2})$	$(2, 2)$
3	$(\sqrt{2}, 2)$	$(\sqrt{2}, \sqrt{2})$	$\dots$	$(2, 0)$	$(2, \sqrt{2})$
4	$(\sqrt{2}, \sqrt{2})$	$(\sqrt{2}, 2)$	$\dots$	$(2, \sqrt{2})$	$(2, 0)$
5	$(2, 0)$	$(2, \sqrt{2})$	$\dots$	$(\sqrt{2}, 2)$	$(\sqrt{2}, \sqrt{2})$
6	$(2, \sqrt{2})$	$(2, 0)$	$\dots$	$(\sqrt{2}, \sqrt{2})$	$(\sqrt{2}, 2)$
7	$(2, 2)$	$(2, \sqrt{2})$	$\dots$	$(\sqrt{2}, 0)$	$(\sqrt{2}, \sqrt{2})$
8	$(2, \sqrt{2})$	$(2, 2)$	$\dots$	$(\sqrt{2}, \sqrt{2})$	$(\sqrt{2}, 0)$

8 tuples for a certain conditional BER are the same each other without considering the order, then the resultant conditional BER becomes the same. For the  $t$ -th bit of user  $\mathbf{c}$ , we define  $\mathcal{T}_{l,m}^{c,t}$  for  $t \in \{1, 2\}$  and  $l, m \in \{1, 2, 3, 4\}$  as a multiset<sup>3</sup> consisting of the 8 tuples  $(|a_i|, |b_i|)$  when  $x_c = s_l$  and  $x_e = s_m$ . Table I summarizes the elements of  $\mathcal{T}_{l,m}^{c,t}$ . It is worth noting that the multisets  $\mathcal{T}_{l,m}^{c,t}$  for all  $t, l$ , and  $m$  are the same as each other, and thus, the resultant conditional BER is the same as each other as well. Hence, the upper bound of the BER in (7) is the upper bound for the unconditional BER of user  $\mathbf{c}$  without loss of generality.

### B. BER of Cell-Edge User

Fig. 2(b) shows the super-imposed QPSK symbols from two users at the BS and the error event of cell-edge user, where we assume that both

<sup>3</sup>A multiset (also known as mset) is a modification of the concept of a set that allows for multiple instances for each of its elements.

users send all zero bits, i.e.,  $x_c = x_e = (1+j)/\sqrt{2}$ . As in the previous subsection, we first consider the BER of the *first* bit among two bits of user  $\mathbf{e}$ , and then show that it is actually the unconditional BER of user  $\mathbf{e}$ . Then, (3) can be rewritten by

$$\Pr(\mathcal{E}|\mathbf{g}_c, \mathbf{g}_e) \leq \sum_{i=1}^8 Q\left(\sqrt{\frac{\tilde{\delta}_i^2}{2N_0}}\right), \quad (8)$$

where  $\tilde{\delta}_i = \|\mathbf{g}_c \tilde{a}_i + \mathbf{g}_e \tilde{b}_i\|$ ,  $\tilde{a}_i = s_1 - s_i$  for  $1 \leq i \leq 4$ ,  $\tilde{a}_i = s_1 - s_{i-4}$  for  $5 \leq i \leq 8$ ,  $\tilde{b}_i = s_1 - s_3$  for  $1 \leq i \leq 4$ , and  $\tilde{b}_i = s_1 - s_4$  for  $5 \leq i \leq 8$ . Then,  $\mathbf{g}_c \tilde{a}_i + \mathbf{g}_e \tilde{b}_i \sim \mathcal{CN}(\mathbf{0}, (P_c d_c^{-\alpha} |\tilde{a}_i|^2 + P_e d_e^{-\alpha} |\tilde{b}_i|^2) \cdot \mathbf{I}_N)$  due to property of complex Gaussian random vector. Let  $\tilde{Z}_i \triangleq \tilde{\delta}_i^2 / (2N_0)$ , and then  $\tilde{Z}_i$  follows Erlang distribution with mean  $N\tilde{\gamma}_i$  and variance  $N\tilde{\gamma}_i^2$ , where

$$\tilde{\gamma}_i = \frac{\rho_c |\tilde{a}_i|^2 + \rho_e |\tilde{b}_i|^2}{2}, \quad (9)$$

$\rho_c = P_c d_c^{-\alpha} / N_0$  and  $\rho_e = P_e d_e^{-\alpha} / N_0$ .

Similarly to (7), we obtain an upper bound of the average BER of user  $\mathbf{e}$  as follows:

$$\begin{aligned} P_{b,e} &\leq \mathbb{E} \left[ \sum_{i=1}^8 Q\left(\sqrt{\tilde{Z}_i}\right) \right] = \sum_{i=1}^8 \mathbb{E} \left[ Q\left(\sqrt{\tilde{Z}_i}\right) \right] \\ &= \sum_{i=1}^8 \frac{1}{2} \left[ 1 - \sum_{k=0}^{N-1} \binom{2k}{k} \sqrt{\frac{1}{1+2/\tilde{\gamma}_i}} \frac{1}{(2\tilde{\gamma}_i+4)^k} \right]. \end{aligned} \quad (10)$$

As we noted before, (10) denotes the BER of user  $\mathbf{e}$ 's first bit given that both users send  $s_1$ . We will show that (10) is actually the unconditional BER of user  $\mathbf{e}$ 's first bit regardless of both  $x_c$  and  $x_e$ . Furthermore, we will show that the second bit of user  $\mathbf{e}$  has the same BER as well.

As in the previous subsection, the BER in (10) depends on  $\tilde{\gamma}_i$ , and then  $\tilde{\gamma}_i$  depends only on a tuple  $(|\tilde{a}_i|, |\tilde{b}_i|)$  for  $i = 1, 2, \dots, 8$ . The bit

TABLE II  
ALL ELEMENTS OF  $\mathcal{T}_{l,m}^{e,t}$

$i$	$\mathcal{T}_{l,m}^{e,t}$				
	$\mathcal{T}_{1,1}^{e,1}$	$\mathcal{T}_{1,2}^{e,1}$	$\dots$	$\mathcal{T}_{4,3}^{e,2}$	$\mathcal{T}_{4,4}^{e,2}$
1	(0, 2)	(0, $\sqrt{2}$ )	$\dots$	( $\sqrt{2}$ , 2)	( $\sqrt{2}$ , 2)
2	( $\sqrt{2}$ , 2)	( $\sqrt{2}$ , $\sqrt{2}$ )	$\dots$	(2, 2)	(2, 2)
3	(2, 2)	(2, $\sqrt{2}$ )	$\dots$	( $\sqrt{2}$ , 2)	( $\sqrt{2}$ , 2)
4	( $\sqrt{2}$ , 2)	( $\sqrt{2}$ , $\sqrt{2}$ )	$\dots$	(0, 2)	(0, 2)
5	(0, $\sqrt{2}$ )	(0, 2)	$\dots$	( $\sqrt{2}$ , $\sqrt{2}$ )	( $\sqrt{2}$ , $\sqrt{2}$ )
6	( $\sqrt{2}$ , $\sqrt{2}$ )	( $\sqrt{2}$ , 2)	$\dots$	(2, $\sqrt{2}$ )	(2, $\sqrt{2}$ )
7	(2, $\sqrt{2}$ )	(2, 2)	$\dots$	( $\sqrt{2}$ , $\sqrt{2}$ )	( $\sqrt{2}$ , $\sqrt{2}$ )
8	( $\sqrt{2}$ , $\sqrt{2}$ )	( $\sqrt{2}$ , 2)	$\dots$	(0, $\sqrt{2}$ )	(0, $\sqrt{2}$ )

error occurs from 8 different error events, each of which depends on the tuple  $(|\tilde{a}_i|, |\tilde{b}_i|)$ . Thus, the another conditional BER when  $x_c$  or  $x_e$  is not equal to  $s_1$  can be derived by obtaining the corresponding tuple  $(|\tilde{a}_i|, |\tilde{b}_i|)$ . If 8 tuples for a certain conditional BER are the same each other without considering the order, then the resultant conditional BER becomes the same. For the  $t$ -th bit of user  $\mathbf{e}$ , we define  $\mathcal{T}_{l,m}^{e,t}$  for  $t \in \{1, 2\}$  and  $l, m \in \{1, 2, 3, 4\}$  as a multiset consisting of the 8 tuples  $(|\tilde{a}_i|, |\tilde{b}_i|)$  when  $x_c = s_l$  and  $x_e = s_m$ . Table II summarizes the elements of  $\mathcal{T}_{l,m}^{e,t}$ . It is worth noting that the multisets  $\mathcal{T}_{l,m}^{e,t}$  for all  $t, l$ , and  $m$  are the same as each other, and thus, the resultant conditional BER is the same as each other as well. Hence, the upper bound of the BER in (10) is the upper bound for the unconditional BER of user  $\mathbf{e}$  without loss of generality.

Using the above union bound approach, the BER performance of the general uplink NOMA system with more than three users and high-order modulation schemes can be analyzed. To be specific, for the uplink NOMA with  $K$  users and  $M$ -QAM scheme, we need to consider  $M^K/2$  error cases by a multiset  $\mathcal{T}_{l,m}^{u,t}$  consisting of  $M^K/2$  tuples to obtain the BER in (7) and (10).

### C. Diversity Order of Two-User Uplink NOMA System

In this section, we analyze diversity order of the two-user uplink NOMA system, which is defined as:

$$\eta_u = - \lim_{\rho_u \rightarrow \infty} \frac{\log P_{b,u}}{\log \rho_u}, \quad \text{for } u \in \{\mathbf{c}, \mathbf{e}\}, \quad (11)$$

which is in general used to capture the behavior of error probability in the high SNR regime [14]. We apply Taylor series expansion to (7) and (10) in order to obtain the diversity order by assuming that the received SNR is high. Then, an asymptotic expression which considers only the first term in Taylor series expansion is obtained by

$$P_{b,u} \approx \beta_{u,N} \rho_u^{-N}, \quad \text{for } u \in \{\mathbf{c}, \mathbf{e}\}, \quad (12)$$

where  $\beta_{u,N}$  denotes the first coefficient of Taylor series expansion for the BER of user  $u$  and varies according to the number of receive antenna at the BS,  $N$ . The term  $\beta_{u,N}$  is numerically obtained and summarized in Table III. Plugging (12) into (11), it is shown that the diversity order of the two-user uplink NOMA system is equal to  $N$ , i.e.,

$$\eta_u = - \lim_{\rho_u \rightarrow \infty} \frac{\log \beta_{u,N} \rho_u^{-N}}{\log \rho_u} = N, \quad \text{for } u \in \{\mathbf{c}, \mathbf{e}\}, \quad (13)$$

which is the same as orthogonal multiple access (OMA) systems with  $N$  receive antennas at the BS. In addition, we observe that both cell-center and cell-edge users have the same diversity order with the joint ML detector.

TABLE III  
VALUES OF  $\beta_{u,N}$  ACCORDING TO  $N$

$N$	$\rho_c = \rho_e$	$\rho_c = 2\rho_e$	$\rho_c = 8\rho_e$		
	$\beta_{c,N} = \beta_{e,N}$	$\beta_{c,N}$	$\beta_{e,N}$	$\beta_{c,N}$	$\beta_{e,N}$
1	1.88	2.33	1.52	2.73	1.02
2	1.61	2.12	1.25	3.08	0.98
3	1.88	2.51	1.55	4.17	1.41
4	2.69	3.46	2.40	6.25	2.33
5	4.36	5.31	4.10	9.97	4.06
6	7.59	8.78	7.36	16.55	7.33
7	13.74	15.23	13.53	28.26	13.51
8	25.44	27.33	25.24	49.20	25.24
9	47.77	50.16	47.58	86.98	47.57
10	90.48	93.54	90.30	155.67	90.30

TABLE IV  
COMPUTATIONAL COMPLEXITY IN TERMS OF COMPLEX NUMBER OPERATION

	Adder	Multiplier	Comparator
SIC	$2M(2N-1)+1$	$4MN$	$2(M-1)$
JML	$M^2(3N-1)$	$3M^2N$	$M^2-1$

### D. Computational Complexity of Joint ML and SIC Detector

In this subsection, we compare the computational complexity of the joint ML and the SIC detector at the receiver in terms of the (complex) number operations such as adder, multiplier, and comparator for two QPSK modulated symbols from both user  $\mathbf{c}$  and user  $\mathbf{e}$ . The computational complexity of the SIC detector is computed as follows, where user  $\mathbf{c}$ 's symbol is first detected, and then user  $\mathbf{e}$ 's symbol is detected. To detect user  $\mathbf{c}$ 's modulated symbol,  $M$  candidates of the received signal need to be generated as  $\mathbf{g}_c x_c \in \mathbb{C}^{N \times 1}$  for  $x_c \in \{s_1, s_2, \dots, s_M\}$ . Then, the Euclidean distances between the received signal,  $\mathbf{y}$ , and  $M$  candidates are calculated, and the candidate with the minimum distance is determined by using comparator, which is the detection process for user  $\mathbf{c}$ 's modulated symbol. After detecting user  $\mathbf{c}$ 's modulated symbol, the SIC detector eliminates the selected candidate (or equivalently detected symbol) from the received signal vector  $\mathbf{y}$ . For detecting user  $\mathbf{e}$ 's modulated symbol,  $M$  candidates are calculated, and the candidate with the minimum distance is determined by using comparator as well, which is the detection process for user  $\mathbf{e}$ 's modulated symbol.

To obtain the computation complexity of the joint ML detector, we summarize the detection procedure in detail as follows. Different from the SIC detector, the joint ML detector determines signals of both user  $\mathbf{c}$  and user  $\mathbf{e}$  simultaneously. Thus, the joint ML detector generates  $M^2$  candidates, which are given by  $\mathbf{g}_c x_c + \mathbf{g}_e x_e \in \mathbb{C}^{N \times 1}$  for  $x_c, x_e \in \{s_1, s_2, \dots, s_M\}$ . Then, the Euclidean distances between the received signal,  $\mathbf{y}$ , and  $M^2$  candidates are calculated, and the candidate with the minimum distance is determined by using comparator, which is the joint detection process for both user  $\mathbf{c}$  and user  $\mathbf{e}$ .

Table IV compares the computational complexity of the joint ML detector with the SIC detector in terms of number of required operations. As expected, the computation complexity of joint ML detector is higher than that of SIC detector. In general, the computational complexity of multiplier is much larger than the complexity of comparator or adder. The joint ML detector requires  $3M/4$  times higher complexity for  $M \geq 2$  in terms of number of multipliers. Note that the modulation order  $M (\geq 2)$  mainly affects the computational complexity of the joint ML detector rather than the number of receive antennas at the

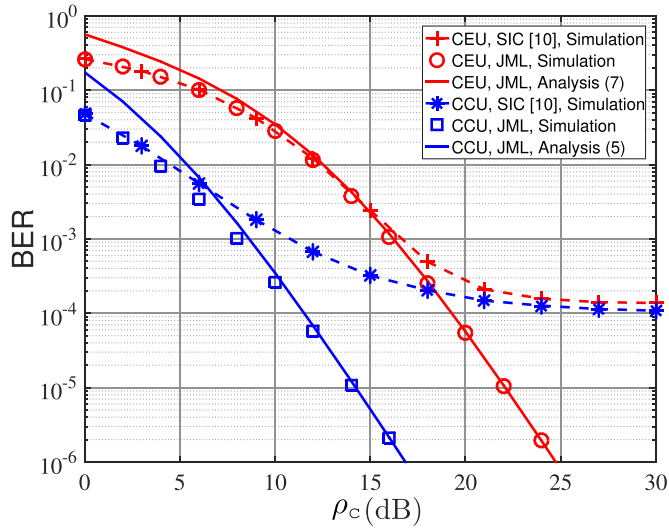


Fig. 3. BER performance of the uplink NOMA system with both JML and SIC receivers for varying SNR when  $N = 4$  and  $\rho_c = 8\rho_e$ .

BS, compared with the complexity of the SIC detector. For example, assuming QPSK at both users and 4 received antennas at the BS, i.e.,  $M = 4$  and  $N = 4$ , the SIC detector requires 57 adder operations, 64 multiplier operations, and 6 comparator operations, while the joint ML detector requires 176 adder operations, 192 multiplier operations, and 15 comparator operations, respectively.

#### IV. NUMERICAL RESULTS

For computer simulations, we define a parameter  $\mu$  as  $\mu = \rho_c/\rho_e$ , which denotes the average received power ratio between the cell-center user (CCU) and the cell-edge user (CEU) at the BS and  $\mu \geq 1$  by definition. Fig. 3 shows the BER performance of the uplink NOMA system with the joint ML (JML) detection technique, compared with the BER with the SIC technique for varying the received SNR values of CCU,  $\rho_c$ , at the BS. We assume that  $\mu = 8$  and the number of antennas at the BS,  $N$ , is equal to 4 in this figure. Due to the fundamental characteristics of the union bound, the BER analysis is not tight for low SNR regime. More specifically, union bound techniques for the BER analysis are based on the summation of exclusive pairwise error probabilities (PEPs), and these PEPs have much intersection area in probability space in the low SNR regime. However, the upper bound of the BER performance in (7) and (10) matches well with the simulation result especially when the received SNR is high. The JML detection technique significantly outperforms the SIC technique in terms of BER performances. With the SIC technique, the BERs of both CCU and CEU become saturated to a similar values as the received SNR increases due to the effect of treating the second user signal as noise at the first user detection (single user detection) [10], even though they result in the same performance as them with the JML detector as the receive SNR is low.

Fig. 4 validates the diversity order analysis in Section III-C for various  $N$ . As expected, the asymptotic analysis expression in (12) tends to approach to upper bound analysis in both (7) and (10). In this figure, the asymptotic analysis is obtained by considering only the highest-degree term in Taylor series expansion. Since the rest (lower-degree) terms in Taylor series are omitted in this figure, the asymptotic results match worse with the simulation results especially when the SNR is low or the number of receive antennas at the BS is large.

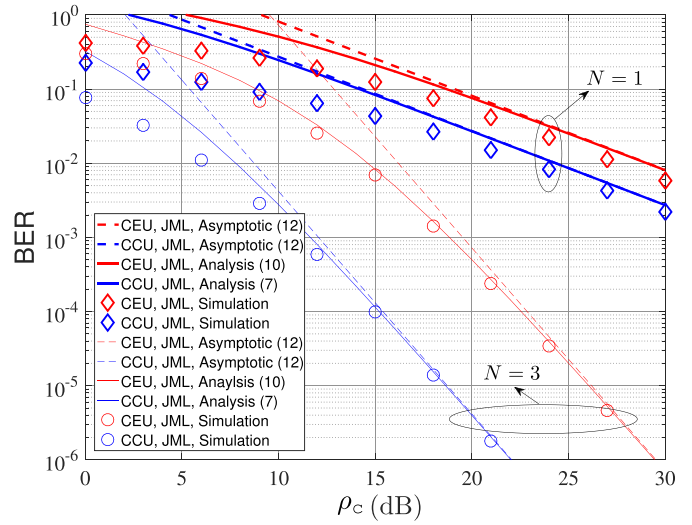


Fig. 4. Diversity order analysis of the uplink NOMA system with the JML detection technique according to  $N$  when  $\rho_c = 8\rho_e$ .

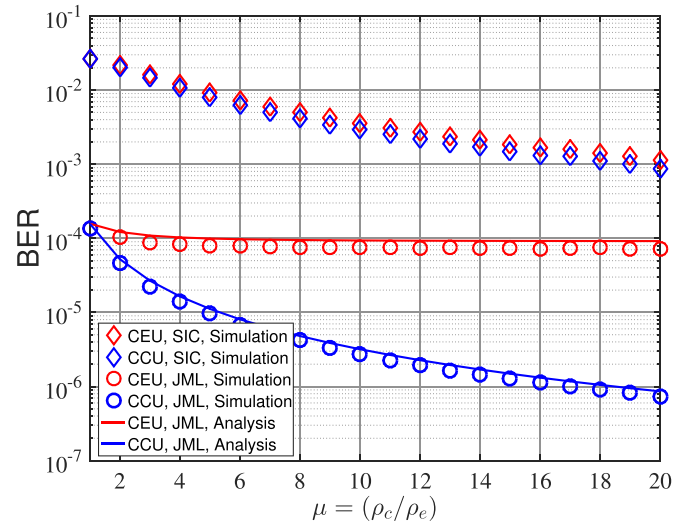


Fig. 5. BER performance of the uplink NOMA system with JML detector and SIC detector according to  $\mu$  when  $N = 2$ .

Fig. 5 shows the BER performance of both CCU and CEU with JML detector and SIC detector at the BS for varying  $\mu$  when the number of receive antennas is equal to 2, which implies the effect of user pairing in the uplink NOMA system on the BER performance. In Fig. 5, we consider the case when  $\rho_e = 20$  dB. The BER performance of CCU becomes improved as  $\mu$  increases since its received SNR increases according to  $\mu$  and the BER performance of CEU becomes also slightly improved even though its received SNR remains constant as  $\mu$  increases. Thus, the user pairing effect of the uplink NOMA system is not significant with the JML detector.

#### V. CONCLUSION

In this paper, the upper bound of bit-error rate (BER) was mathematically characterized in two-user uplink non-orthogonal multiple access (NOMA) system with joint maximum-likelihood detector at a multi-antenna base station (BS). Quadrature phase shift keying (QPSK)

modulation is assumed to be sent from the users who are assumed to be located with arbitrary distance from the BS in a cell. It was shown that the analytical results match well with the computer simulation results especially when signal-to-noise ratio (SNR) is high. In addition, the joint ML detector significantly outperforms the conventional successive interference cancellation (SIC) detector in terms of the BER performance. Diversity order of the joint ML detector was also derived for the uplink NOMA system, and the computational complexity of the joint ML detector was compared with that of the SIC detector, which is the first theoretical result in literature. Our analysis can be extended to general uplink NOMA scenarios with more than three users and  $M$ -QAM schemes. We leave the BER analysis of downlink NOMA systems with the joint ML detector for further study.

#### REFERENCES

- [1] L. Dai, B. Wang, Y. Yuan, S. Han, C.-L. I, and Z. Wang, "Non-orthogonal multiple access for 5G: Solutions, challenges, opportunities, and future research trends," *IEEE Commun. Mag.*, vol. 53, no. 9, pp. 74–81, Sep. 2015.
- [2] Z. Ding *et al.*, "Application of non-orthogonal multiple access in LTE and 5G networks," *IEEE Commun. Mag.*, vol. 55, no. 2, pp. 185–191, Feb. 2017.
- [3] Y. Chen *et al.*, "Toward the standardization of non-orthogonal multiple access for next generation wireless networks," *IEEE Commun. Mag.*, vol. 56, no. 3, pp. 19–27, Mar. 2018.
- [4] Z. Ding, Z. Yang, P. Fan, and H. V. Poor, "On the performance of non-orthogonal multiple access in 5G systems with randomly deployed users," *IEEE Signal Process. Lett.*, vol. 21, no. 12, pp. 1501–1505, Dec. 2014.
- [5] N. Zhang, J. Wang, G. Kang, and Y. Liu, "Uplink non-orthogonal multiple access in 5G systems," *IEEE Commun. Lett.*, vol. 20, no. 3, pp. 458–461, Mar. 2016.
- [6] Z. Ding, R. Schober, and H. V. Poor, "A general MIMO framework for NOMA downlink and uplink transmission based on signal alignment," *IEEE Trans. Wireless Commun.*, vol. 15, no. 6, pp. 4438–4454, Jun. 2016.
- [7] T. Hou, X. Sun, and Z. Song, "Outage performance for non-orthogonal multiple access with fixed power allocation over Nakagami- $m$  fading channels," *IEEE Commun. Lett.*, vol. 22, no. 4, pp. 744–747, Apr. 2018.
- [8] X. Wang, F. Labeau, and L. Mei, "Closed-form BER expressions of QPSK constellation for uplink non-orthogonal multiple access," *IEEE Commun. Lett.*, vol. 21, no. 10, pp. 2242–2245, Oct. 2017.
- [9] J. S. Yeom, E. Chu, B. C. Jung, and H. Jin, "Performance analysis of diversity-controlled multi-user superposition transmission for 5G wireless networks," *MDPI Sensors*, vol. 18, no. 2, Feb. 2018, Art. no. 536.
- [10] F. Kara and H. Kaya, "BER performances of downlink and uplink NOMA in the presence of SIC errors over fading channels," *IET Commun.*, vol. 12, no. 15, pp. 1834–1844, Sep. 2018.
- [11] M. Al-Imari, P. Xiao, M. A. Imran, and R. Tafazolli, "Uplink non-orthogonal multiple access for 5G wireless networks," in *Proc. 11th Int. Symp. Wireless Commun. Syst.*, Aug. 2014, pp. 781–785.
- [12] J. Bao, Z. Ma, G. K. Karagiannidis, M. Xiao, and Z. Zhu, "Joint multiuser detection of multidimensional constellations over fading channels," *IEEE Trans. Commun.*, vol. 65, no. 1, pp. 161–172, Jan. 2017.
- [13] L. Yu, P. Fan, D. Cai, and Z. Ma, "Design and analysis of SCMA codebook based on star-QAM signaling constellations," *IEEE Trans. Veh. Technol.*, vol. 67, no. 11, pp. 10543–10553, Nov. 2018.
- [14] D. Tse and P. Viswanath, *Fundamentals of Wireless Communication*. Cambridge, U.K.: Cambridge Univ. Press, 2005.
- [15] A. Papoulis and S. U. Pillai, *Probability Random Variables and Stochastic Processes*, 4th ed. New York, NY, USA: McGraw-Hill, 2002.